

Thermodynamic Measurements in Pulsed Magnetic Fields

Ramzy Daou, Franziska Weickert¹, Michael Nicklas, and Frank Steglich

Pulsed magnets provide the highest available magnetic fields for research. Non-destructive pulsed magnets that discharge a capacitor through an inductive load are routinely used to reach fields above 60 Teslas, and ever-higher fields are being targeted by a handful of laboratories around the world. The Dresden High Magnetic Field Laboratory (HLD) is one such cutting edge research facility [1]. Founded in 2003 [2], the HLD opened to users in 2007 and forms part of the Euromagnet network of high field laboratories. The Max Planck Society is integrated with the HLD at the ground level through the research program “Materials Science and Condensed Matter Research at the Hochfeld-Magnetlabor Dresden”, based at the MPI-CPfS [3].

Measurements in pulsed magnetic fields are subject to strong constraints that arise both from the short timescale of the experiments (some milliseconds) and the mechanical and electrical noise induced by the rapid discharge of the capacitors. It has therefore been difficult to explore thermodynamic properties of materials with high resolution; even measurements of basic transport properties are challenging.

We have developed two thermodynamic probes for use in the pulsed magnetic fields which boast world-leading resolution. The specific heat experiment utilizes the adiabatic method with specific adaptations for pulsed-field work and the option for carrying out magnetocaloric effect measurements. The magnetostriction experiment sidesteps many of the limitations of the noisy environment by utilizing a novel optical method borrowed from the telecommunications industry. In the following we will present each method and some preliminary results on materials of interest.

Specific heat measurements in pulsed fields

The specific heat is a fundamental thermodynamic quantity in condensed matter physics and probes the change of entropy as a function of temperature. It has a sensitive and characteristic response to changes of the internal free energy, which occur e.g. at phase transitions or when energy levels of

the system are thermally or quantum-mechanically excited. In materials where the entropy shows a sharp discontinuity as a function of the magnetic field, a rapid change in the temperature can be observed while sweeping the field. This effect is called magnetocaloric effect (MCE) and it is a particular useful tool to track phase boundaries in an easy and reliable way. Both techniques the specific heat and the MCE measurements can be realized with essentially the same experimental set-up based on the semi-adiabatic method, where the heater, sample and thermometer are as much as possible thermally decoupled from the environment.

Figure 1 shows the physical arrangement of our experiment including a sample of the isolated spin-1/2 compound AgVOAsO_4 [4]. Unlike a more conventional experiment, there is no sample platform involved. Instead the heater, sample and thermometer are glued together with a tiny amount of GE-varnish in a “sandwich” configuration. The dimensions of this set-up need to be extremely small that the

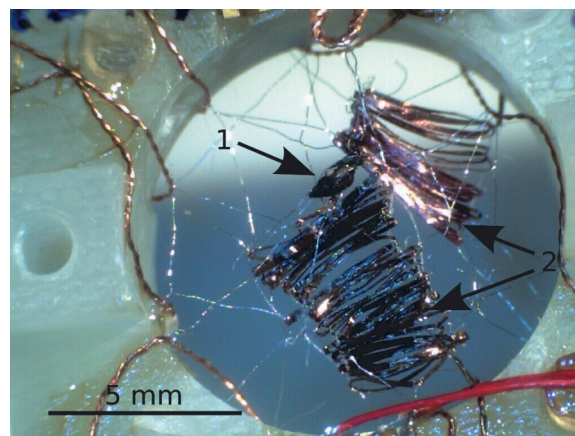


Fig. 1: Experimental set-up for specific heat and MCE measurements. In the centre of the image, the sandwich made of heater, sample and thermometer can be seen (1). Two sets of 6 (15 cm long) thermally resistive constantan wires (2) are used to measure the ruthenium oxide thick film thermometer and to drive the current of the thin film heater without causing a heat leak. Mechanical support and stability is provided by the network of platinum-tungsten wires (silver colored), which also have a low thermal conductivity. The whole sample holder is made of G10 to avoid eddy current heating in pulsed magnetic fields.

time constant of the measurement is shorter than the pulsed field scale. However, the specific heat of the sample should be the dominant contribution compared to the total specific heat including addenda. In the set-up in Figure 1, the thermometer and heater had a mass of 0.1 mg each, while the sample mass was 1.5 mg. The challenge for calorimetric measurements in particular is the implementation of reliable, reproducible thermometry. Resistive thermometers are at present the only viable option as they satisfy the constraints of size, speed and ease of measurement. We were using RuO₂ thick film thermometers with a susceptible temperature response between 20 K and 1.4 K and a small positive magnetoresistance of 7% up to 60 T. However, a careful calibration of the RuO₂-sensor in field is essential before starting the experiment.

Figure 2 shows a characteristic time profile of an experiment carried out at 31 T in the *long-pulse magnet*. This magnet produces a field profile with a rise time of 150 ms, a period of around 100 ms at maximum field ± 1 T and a fall time of 1.5 s. The maximum field currently available at HLD is around 47 T. In the 100 ms time window at the maximum field it is possible to apply several heat pulses of a few ms length and to track simultaneously the adiabatic temperature response of the sample. Hereby the “sandwich” configuration ensures that the heat flow goes through the sample and increases the temperature by about $\Delta T = 0.15$ K. The heater as well as the thermometer are wired with a loop-free 6 wire tape, which enables conventional 4-probe AC (5 kHz) resistivity measurements of the thermometer and a precise monitoring of the applied heat $\Delta Q = \Delta t \times U \times I = 1.7 \mu\text{J}$ in the heater.

Quantum magnets are a family of materials which display phase transitions in high fields as a result of induced spin-reorientations. One particular phase transition of interest is the so-called Bose-Einstein condensation (BEC) of magnons. In the newly discovered quantum spin system AgVOAsO₄ [4] field-induced ordering is observed between 10.5 T and 48 T. We were able to explore the phase diagram of this material via MCE measurements in pulsed magnetic fields. Specific heat data taken in a couple of magnet pulses agree within the error bars (10%) with data taken on the same compound in high DC-magnets (up to 30 T) at the Grenoble High Magnetic Field Laboratory [5].

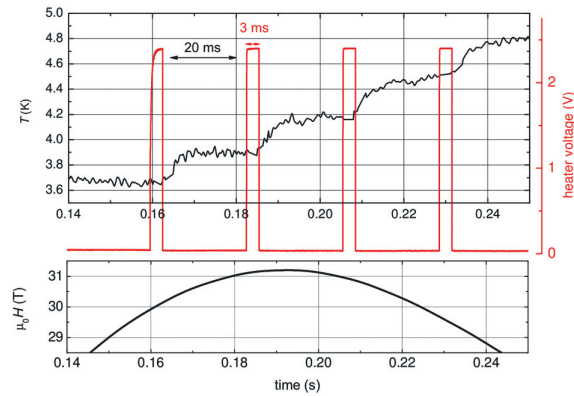


Fig. 2: Typical time scale of a specific heat experiment in the *long-pulse magnet*. The lower panel shows the field profile around the magnetic pulse maximum. In the upper panel the temperature of the sample thermometer is displayed. As short heat pulses are applied (the red curve shows the heater voltage), clear steps in the temperature are observed. The temperature as a function of time between 2 heat pulses shows clearly that i) the time constant of the experiment is well below 10 ms, because the temperature saturates and that ii) the “sandwich” configuration is (on this ms time scale) thermally decoupled from the bath, because the temperature stays stable after reaching its saturation value.

Magnetostriction measurements using Fibre Bragg Gratings

The magnetostriction of a material gives us information about the coupling between magnetism and the lattice. There are many microscopic sources of magnetostrictive effects, foremost among which are exchange interactions between local moments and itinerant electron magnetism. By a convenient Maxwell relation, we know that magnetostriction is equivalent to the pressure dependence of the magnetization. It is also a directional probe that can be used to explore anisotropic magnetic interactions. Integrating a sensitive magnetostriction measurement with pulsed magnetic fields allows us to access magnetic interactions at higher energy scales than is possible in conventional laboratory magnets.

We have developed a technique to measure magnetostriction in pulsed fields [6] that provides an improvement in resolution of two orders of magnitude over previous methods [7]. We utilize a technology from the telecommunications industry known as a Fiber Bragg Grating (FBG). A periodic modulation of the refractive index in the core of an optical fiber over some short length introduces a

peak in the reflectivity spectrum of the fiber at a wavelength dependent on the period of the modulation. This structure can then be used as a sensitive strain gauge, as the wavelength of reflection shifts linearly with the strain applied to the fiber. Such an FBG is attached to the side of the sample of interest with cyanoacrylate glue. The fiber is then illuminated with broadband light and the reflection is collected by a spectrometer with a very fast camera capable of acquiring complete spectra at 47 kHz. It is this camera that allows us to obtain both the required sensitivity and sufficient time resolution to make pulsed field experiments feasible.

The main advantage of this technique is that it is optically based and is therefore immune to electromagnetic noise which can be a severe problem in pulsed magnets. Since the FBG is used as a strain gauge and is fixed directly to the sample (which is itself glued to the measurement probe), it also confers some immunity from mechanical vibrations. The magnetic field dependence of the FBG response is also well understood and independent of temperature, unlike for example a resistive foil strain gauge whose magnetoresistance must be carefully calibrated in the pulsed field before use [8]. Finally, it is simply attached and detached from the sample with an everyday glue.

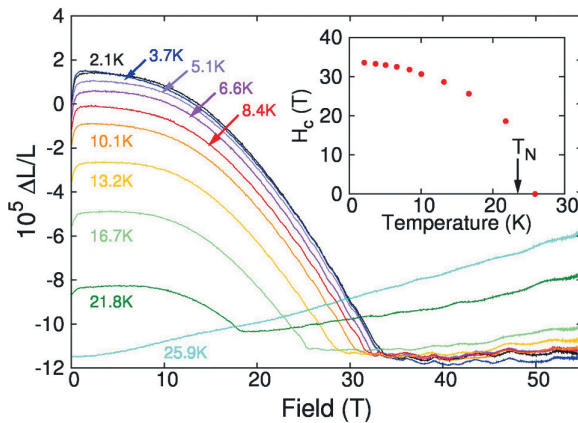


Fig. 3: Longitudinal magnetostriction of a single crystal of GdSb measured by FBG method in pulsed fields up to 54 T ($\Delta L \parallel B \parallel a$) [4]. The curves are offset by the relative thermal expansion of the sample. At high fields and low temperatures, quantum oscillations of the magnetostriction can be observed. The sample length decreases as antiferromagnetism is suppressed, and then saturates when the saturation magnetisation is reached. *Inset*: the magnetic phase diagram extracted from the main panel. The red dots mark the antiferromagnetic/paramagnetic phase boundary corresponding to the shoulder in the magnetostriction.

The success of this technique is illustrated by Figure 3 and 4. In Figure 3 we see the longitudinal magnetostriction of GdSb, an antiferromagnetic semimetal. The Gd lattice orders below 23 K and a field of 33 T is required to suppress this and fully polarize the lattice. Meanwhile, at high fields the itinerant quasiparticles cause quantum oscillations in the magnetostriction [9]. To our knowledge, this is the first observation of quantum oscillations in the magnetostriction in fields above 33 T. The resolution of the measurement is $\Delta L/L \approx 3 \times 10^{-7}$ at 47 kHz, which represents an improvement of around two orders of magnitude over the plastic capacitance dilatometer of Ref. [7] which achieved a resolution of 10^{-5} at 10 kHz.

Figure 4 shows the longitudinal magnetostriction of the quantum magnet $\text{SrCu}_2(\text{BO}_3)_2$. This compound consists of orthogonally oriented spin-dimers on a square lattice. This arrangement is a near-perfect realization of the theoretical Hamiltonian written down by Shastry and Sutherland [10], whereby two orthogonal exchange interactions of similar magnitude cause strong geometrical frustration. The ground state consists of spin-

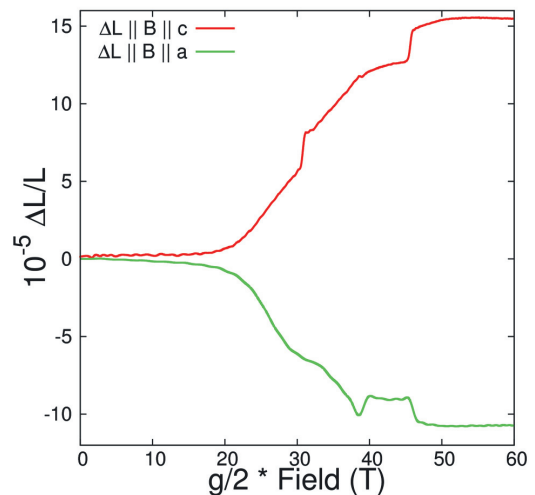


Fig. 4: Magnetostriction of $\text{SrCu}_2(\text{BO}_3)_2$ measured in pulsed fields up to 60 T at the HLD for fields applied in both in and perpendicular to the dimer planes. The data have been scaled by the electronic g -factor appropriate to the field direction. The length change of the sample shows different steps and plateaux corresponding to long-range ordered states when the number of triplet excitations that form on the dimers is a rational fraction of the total number. Unlike the magnetization, which is positive and always increases with field for both directions, the magnetostriction has varying sign for each step, corresponding to the different uniaxial pressure dependencies of each magnetic phase.

singlets states on each dimer, but as the spin-gap is closed with strong fields of around 20 T, triplet excitations are formed. It is thought that at integer fractions of the saturation magnetization, long range order of these triplet excitations is stabilized in structures that are commensurate with the lattice. This is manifested in steps and plateaux in the magnetization which have been much studied [11,12].

As Figure 4 shows, these steps are also present in the magnetostriction. What is qualitatively new, however, is that while the magnetization is nearly identical for magnetic fields applied within the plane of the dimers and perpendicular to it, the magnetostriction is dramatically different. Since the magnetostriction is equivalent to the uniaxial pressure derivative of the magnetization, it suggests a qualitatively different response of the exchange parameters to pressure applied in the plane and perpendicular to it, and of the different compressibilities of the long range ordered phases, some of which appear much stiffer than others. This behavior must be accounted for by numerical and theoretical models that attempt to describe the interplay between dimers quantitatively.

Summary

We have developed thermodynamic probes for use in pulsed magnetic fields and improved their resolution to the point where new physics can be explored. These techniques complement and extend the range of available probes that can be

used in the challenging, but uniquely capable environment of pulsed magnetic fields and are now open to users of the facility.

This study was partly supported by EuroMagNetII under EU contract 228043 and by the MPG Research Initiative “Materials Science and Condensed Matter Research at the Hochfeld-Magnetlabor Dresden.”

References

- [1] *S. Zherlitsyn et al.*, IEEE **20** (2010) 672.
- [2] *Max Planck Institute for Chemical Physics of Solids*, Scientific Report 2001/2002 (2003).
- [3] *Max Planck Institute for Chemical Physics of Solids*, Scientific Report 2003-2005 (2006).
- [4] *A. A. Tsirlin et al.*, arXiv: 1101.2546v1.
- [5] *Unpublished results.*
- [6] *R. Daou et al.*, Rev. Sci. Instrum. **81** (2010) 033909.
- [7] *M. Doerr et al.*, Rev. Sci. Instrum. **79**, (2008) 063902.
- [8] *P. A. Algarabel, A. del Moral, C. Mart, D. Serrate, and W. Tokarz*, J. Phys.: Conference Series **51** (2006) 607.
- [9] *R. Daou et al.*, J. Phys.: Conf. Ser. **273** (2011) 012111.
- [10] *S. Shastry and W. Sutherland*, Phys. Rev. Lett. **47** (1981) 964.
- [11] *S. Sebastian et al.*, Proc. Nat. Acad. Sci. **105** (2008) 20157.
- [12] *M. Takigawa et al.*, J. Phys. Soc. Jpn. **79** (2010) 011005.

¹ Present address: Los Alamos National Laboratory, Los Alamos, NM 87545, United States